Shifting Interpolation Kernel Toward Orthogonal Projection

Bashir Sadeghi, *Student Member, IEEE*, Runyi Yu, *Senior Member, IEEE*, and Ruili Wang

***Abstract*—Orthogonal projection offers the optimal solution for many sampling-reconstruction problems in terms of the least square error. In the standard interpolation setting where the sampling is assumed to be ideal, however, the projection is impossible unless the interpolation kernel is related to the sinc function and the input is bandlimited. In this paper, we propose a notion of shifting kernel toward the orthogonal projection. For a given interpolation kernel, we formulate optimization problems whose solutions lead to shifted interpolations that, while still being interpolatory, are closest to the orthogonal projection in the sense of the minimax regret. The quality of interpolation is evaluated in terms of the average approximation error over input shift. For the standard linear interpolation, we obtain several values of optimal shift, dependent on *a priori* information on input signals. For evaluation, we apply the new shifted linear interpolations to a Gaussian signal, an ECG signal, a speech signal, a two-dimensional signal, and three natural images. Significant improvements are observed over the standard and the 0.21-shifted linear interpolation proposed early.**

***Index Terms*—Approximation error, interpolation kernel, kernel shifting, minimax regret sampling, orthogonal projection.**

I. Introduction

ORTHOGONAL projection offers the optimal solution for many inverse problems such as interpolation and reconstruction. Its realization, however, imposes strict conditions on the corresponding processes. For example, for generalized sampling and reconstruction processes, the reconstruction subspace is required to be a subspace of the sampling subspace [10]. In the standard interpolation setting where the sampling is assumed to be ideal, the orthogonal projection is impossible unless the interpolation kernel is associated with the sinc function and the input is bandlimited.

On the other hand, in spite of development of many interpolation methods [3], [7], [14], the linear interpolation remains by far the most popular solution for many applications including image processing such as digital photography and image resampling [3]. In comparison with other interpolation kernels, the linear kernel has a very simple form (thus is easy for hardware implementation); yet it enjoys reasonably good quality [15].

It has been shown [16] that there is significant room for improvement of the linear interpolation toward the orthogonal projection. One approach for such improvement is to shift the linear kernel [3]. In the limiting sampling case, it has been shown that the 0.21-shifted linear interpolation can achieve an asymptotic error that is very close to the error of the orthogonal projection.

Note that the assumption of limiting sampling is rather restrictive; it requires that frequency content of the signal be primarily concentrated around the zero frequency. When the sampling period is not very small, especially when the continuous-time signal contains significant components around the Nyquist frequency, the asymptotic error is no more appropriate to be used to evaluate the quality of approximation as demonstrated by the examples in [20]. Instead, an estimate of the approximation error was used in [20] to design optimized quasi-interpolations, although only a portion of the Nyquist band is considered in the estimate. Furthermore, exploiting high frequency information is crucial to many edge-based reconstructions such as in image-zooming [5] and super-interpolation [6].

In this paper, we use the average approximation error over input shift as the quality measure for interpolation schemes. According to [4], the quality of approximation can be adequately evaluated in terms of the average error, especially when the initial time is not precise. And this average error, closely related to the shift-variance of the processes [18], [30], can be characterized in terms of an error kernel and the input signal. This characterization includes contents of the input beyond the Nyquist frequency.

Our aim is to minimize the average approximation error by shifting the interpolation kernel. Since the orthogonal projection is optimal and cannot be achieved by any kernel except the sinc function, we propose to shift the kernel toward approaching this optimal solution. We recall that the idea of kernel shifting was initiated in [17] for the stability of interpolation operators. It was also used in [3] to improve the asymptotic interpolation error. To our best knowledge, the work in this paper is the first attempt to exploit kernel shifting toward orthogonal projection. It is in the spirit of the minimax regret sampling [10] but with the requirement that the sampling be interpolatory, thus consistent [25]. Since our target is the orthogonal projection, we assume that in the minimax regret sampling the input signal is bandlimited by the Nyquist frequency.

Manuscript received February 10, 2017; revised July 4, 2017 and August 14, 2017; accepted September 11, 2017. Date of publication October 2, 2017; date of current version November 13, 2017. The associate editor coordinating the review of this manuscript and approving it for publication was Dr. Eleftherios Kofidis. *(Corresponding author: Runyi Yu.)*

B. Sadeghi and R. Yu are with the Department of Electrical and Electronic Engineering, Eastern Mediterranean University, Gazimagusa, via Mersin 10 99628, Turkey (e-mail: bashir@ieee.org; yu@ieee.org).

R. Wang is with the Institute of Natural and Mathematical Sciences, Massey University, Auckland 0745, New Zealand (e-mail: r.wang@massey.ac.nz).

Color versions of one or more of the figures in this paper are available online at http://ieeexplore.ieee.org.

Digital Object Identifier 10.1109/TSP.2017.2759100

Moreover, we exemplify our theory with the linear B-spline kernel [23]. In this particular case, we obtain two values of shift, namely, 1/11 and 1/8. We show that when no *a priori* knowledge on the continuous-time input is available, the 1/11-shifted linear interpolation will generally produce near-optimal interpolation. This is also the case for signals in shiftable subspaces generated by B-splines. On the other hand, the 1/8-shifted linear interpolation would tend to yield good results for signals in Sobolev subspace and for signals arisen from natural images.

To evaluate performance of the shifted linear interpolation, we apply shifted linear interpolations to a Gaussian signal, an ECG signal, a speech signal, a 2-dimensional signal, and three natural images. Significant improvements are observed over the standard linear interpolation and the 0.21-shifted linear interpolation proposed in [3].

The main contributions of this paper is as follows:

1) We propose to shift the kernel to achieve a sampling scheme that is both interpolatory and closest to the orthogonal projection in the minimax regret sense.
2) We provide a method for analyzing optimal kernel shifting in terms of the average approximation error.
3) We carry out detailed study on the standard linear kernel, and we obtain two values of shift for near-optimal shift.

The remainder of the paper is organized as follows. In Section II, we review orthogonal projection on shiftable subspaces and present its average approximation error to be used as a benchmark. Linear interpolation, minimax regret sampling, and kernel shifting are introduced in Section III. In Section IV, we propose optimization problems for shifting kernel, and obtain solutions for the linear kernel. We propose and solve a minimax regret optimization that pulls the shifted-interpolation toward orthogonal projection in Section V. Section VI describes some experiments. Finally, conclusions are drawn in Section VII.

The notation is quite standard. $\mathbb{Z}$ and $\mathbb{R}$ are the set of integers and of real numbers, respectively. We use L^1 and L^2 to denote, respectively, the space of absolute integrable (continuous-time) signals and the Hilbert space of square integrable signals. For $x \in L^2$, its norm is given by $\|x\|_2^2 = \int_{\mathbb{R}} |x(t)|^2 \,\mathrm{d}t$. The Fourier transform is indicated by the hat sign "$\widehat{\ }$", e.g., $\widehat{x}(\omega) = \int_{\mathbb{R}} x(t)\, e^{-j\omega t} \,\mathrm{d}t$ for signal x which is also denoted by $x(\cdot)$. Throughout the paper, all signals are assumed to be real-valued. Thus, $|\widehat{x}(\omega)| = |\widehat{x}(-\omega)|, \omega \in \mathbb{R}$. The symbol "$*$" is the convolution operator.

II. Orthogonal Projection and Average Error

Let $T > 0$ be a sampling period and $w \in L^1 \cap L^2$ be a generator for the T-shiftable closed subspace

$$\mathcal{W} = \left\{ x_r : x_r(t) = \sum_{n\in\mathbb{Z}} c_n w\left(\frac{t}{T} - n\right), \{c_n\} \in \ell^2 \right\}.$$

We assume that $\{w(\frac{\cdot}{T} - n)\}_{n\in\mathbb{Z}}$ constitutes a frame of $\mathcal{W}$ [28]. When used in interpolation, w is usually called an interpolation kernel (or reconstruction kernel).

Let $P_{\mathcal{W}}$ be the orthogonal projection on $\mathcal{W}$. It is well-known that $P_{\mathcal{W}}$ gives the optimal solution in the least square framework. Specifically, for any given $x \in L^2$, $P_{\mathcal{W}}x$ is the unique solution to the least square error problem

$$\min_{y\in\mathcal{W}} \|x - y\|_2^2. \tag{1}$$

In view of the uncertainty with the initial time of signals, the quality of this approximation can be adequately evaluated in terms of the average error (with respect to input shift in one sampling period) defined by [3], [4]

$$e_x^2 = \frac{1}{T}\int_0^T \|(I - P_{\mathcal{W}})x(\cdot - s)\|_2^2 \,\mathrm{d}s \tag{2}$$

where $I : L^2 \longrightarrow L^2$ is the continuous-time identity operator, $x(\cdot - s)$ is the s-shifted version of signal $x(\cdot)$. In the Fourier domain, e_x^2 can be expressed [4] by

$$e_x^2 = \int_{\mathbb{R}} E_P(\omega) \left|\widehat{x}\left(\frac{\omega}{T}\right)\right|^2 \frac{\mathrm{d}\omega}{2\pi T} \tag{3}$$

where E_P is the so-called error kernel of the orthogonal projection:

$$E_P(\omega) = 1 - \frac{|\widehat{w}(\omega)|^2}{\sum_{n\in\mathbb{Z}} |\widehat{w}(\omega + 2\pi n)|^2}. \tag{4}$$

For kernel w with finite support in time, the infinite summation in the denominator may be further simplified by applying the Poisson summation formula [28] to the convolution $w * w(-\cdot)$:

$$\sum_{n\in\mathbb{Z}} |\widehat{w}(\omega + 2\pi n)|^2 = \sum_{n\in\mathbb{Z}} (w * w(-\cdot))(n)\, e^{-jn\omega}. \tag{5}$$

Since the orthogonal projection is optimal, the kernel E_P can serve as a benchmark for approximation quality evaluation of sampling schemes.

As a particular example, let the interpolation kernel be the linear B-spline (hat) function:

$$w(t) = \beta(t) = \begin{cases} 1 - |t|, & |t| < 1 \\ 0, & \text{otherwise} \end{cases} \tag{6}$$

whose Fourier transform is given by

$$\widehat{w}(\omega) = \mathrm{sinc}^2\left(\frac{\omega}{2\pi}\right) = \left(\frac{\sin(\omega/2)}{\omega/2}\right)^2. \tag{7}$$

Since $(w * w(-\cdot))(t) = \beta^3(t)$ (the B-spline of order 3, which becomes zero if $|t| \geq 2$) [26], it follows from (5) that

$$\sum_{n\in\mathbb{Z}} |\widehat{w}(\omega + 2\pi n)|^2 = \sum_{n=-1}^{1} \beta^3(n) e^{-jn\omega} = \frac{1}{3}(2 + \cos\omega). \tag{8}$$

As a result, the error kernel for the linear B-spline becomes

$$E_P(\omega) = 1 - \frac{3\,\mathrm{sinc}^4\left(\frac{\omega}{2\pi}\right)}{2 + \cos\omega}. \tag{9}$$

This benchmark kernel is plotted in Fig. 1.

III. Interpolation and Kernel Shifting

In this section, we present the notion of kernel shifting toward orthogonal projection.

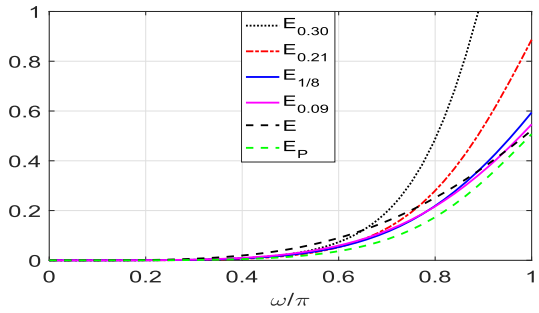

Fig. 1. Error kernels: E_P of the orthogonal projection, E of the standard linear interpolation, and E_τ of the τ-shifted linear interpolation ($\tau = 0.09, 1/8, 0.21, 0.30$).

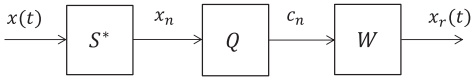

Fig. 2. The standard interpolation scheme.

A. Interpolation and Correction Filter

The standard interpolation is illustrated in Fig. 2. Given an input signal $x \in L^2$, the ideal sampling operator $S^* : L^2 \to \ell^2$ (of kernel δ, the dirac sequence) [10] with sampling period T yields a discrete-time sequence:

$$S^* : x(t) \mapsto \{x_n\} = \{x(nT)\}.$$

By combining the time-scaled and time-shifted versions of the kernel w, the synthesis operator W generates a continuous-time signal given below:

$$W(\ell^2 \to \mathcal{W}) : c = \{c_n\} \mapsto x_r(t) = \sum_{n\in\mathbb{Z}} c_n\, w\left(\frac{t}{T} - n\right).$$

The coefficients used to generate x_r do not need to be the same as the samples given by S^*. As a matter of fact, they can be modified by a (linear shift-invariant) correction filter Q:

$$Q\ (\ell^2 \to \ell^2) : c \mapsto c * q$$

where sequence $q = \{q_n\}$ is the impulse response of filter Q.

Suppose that it is required the sampling be interpolatory, that is, the reconstruction x_r should keep the values of input x at the sampling instants, i.e., $x_r(nT) = x(nT), n \in \mathbb{Z}$. Then the sampling becomes consistent [25]. The interpolatory sampling can be achieved by the correction filter [3]

$$\widehat{q}(e^{j\omega}) = \frac{1}{W(e^{j\omega})} \tag{10}$$

where

$$W(e^{j\omega}) = \sum_{n\in\mathbb{Z}} \widehat{w}(\omega + 2\pi n) = \sum_{n\in\mathbb{Z}} w_n e^{-jn\omega}. \tag{11}$$

The last equality is from the Poisson's summation formula [28]. Here, for the stability of the filter Q, it is assumed that the infimum of the magnitude of W is greater than zero.

As in the case of orthogonal projection, the quality of the interpolation of Fig. 2 can be adequately evaluated in terms of the average error:

$$e_x^2 = \frac{1}{T}\int_0^T \|(I - WQS^*)x(\cdot - s)\|_2^2\, \mathrm{d}s. \tag{12}$$

According to [4] (or [19] for a system theory derivation), e_x^2 can also be expressed in the Fourier domain by

$$e_x^2 = \int_{\mathbb{R}} E(\omega) \left|\widehat{x}\left(\frac{\omega}{T}\right)\right|^2 \frac{\mathrm{d}\omega}{2\pi T} \tag{13}$$

where E is the error kernel of the interpolation process in Fig. 2 and is given as

$$E(\omega) = |1 - \widehat{q}(e^{j\omega})\widehat{w}(\omega)|^2 + |\widehat{q}(e^{j\omega})|^2 \sum_{n\neq 0} |\widehat{w}(\omega + 2\pi n)|^2. \tag{14}$$

Note that the second term in the right-hand side of (14) is actually the shift-variance kernel, which characterizes variance of the error due to input shift [19].

The error kernel can also be reorganized to become

$$E(\omega) = 1 + |\widehat{q}(e^{j\omega})|^2 \sum_{n\in\mathbb{Z}} |\widehat{w}(\omega + 2\pi n)|^2 - 2\mathrm{Re}\left(\widehat{q}(e^{j\omega})\widehat{w}(\omega)\right). \tag{15}$$

Then, the infinity summation term can be computed using (5).

In the case of linear interpolation, the reconstruction kernel is $w(t) = \beta(t)$, thus $w_n = w(nT/T) = \beta(n) = \delta_n$ in view of (6). Then from (10) and (11), it follows $\widehat{q}(e^{j\omega}) = 1, \omega \in \mathbb{R}$. That is, Q specializes to the discrete-time identity operator. This implies that the standard linear interpolation is consistent in itself. In other words, the samples x_n can be directly used in the reconstruction without resulting in error at sampling instants.

In addition, from (15), (7), and (5), it follows that

$$E(\omega) = \frac{1}{3}(5 + \cos\omega) - 2\,\mathrm{sinc}^2\left(\frac{\omega}{2\pi}\right) \tag{16}$$

which is also plotted in Fig. 1 for comparison.

It is worthy pointing out that for the linear interpolation kernel, the orthogonal projection cannot be realized by the sampling scheme of Fig. 2 if S^* is the ideal sampling operator, regardless of the correction filter Q used.

B. Minimax Regret Sampling and Kernel Shifting

Although being consistent, the interpolation can produce very large error [10]. One approach to overcome this drawback is the scheme of minimax regret sampling [10], [11]. Through correction filter Q, this scheme aims to minimize the difference between the instantaneous approximation error and the optimal error obtained by the orthogonal projection:

$$\min_{Q} \max_{\|x\|_2 \le 1} \left\{\|(I - WQS^*)x\|_2^2 - \|(I - P_{\mathcal{W}})x\|_2^2\right\}.$$

It is essentially pulling the sampling scheme toward the orthogonal projection, since

$$\|(I - WQS^*)x\|_2^2 - \|(I - P_{\mathcal{W}})x\|_2^2 = \|WQS^*x - P_{\mathcal{W}}x\|_2^2.$$

Unfortunately, this scheme generally results in value changes at sampling instants. This implies that when it is used in zooming-in and zooming-out processes, it cannot bring back original digital displays.

We shall now show that this shortcoming can be circumvented by shifting the reconstruction kernel w.

Let τ be the amount of the shift, $w_\tau(\cdot) = w(\cdot - \tau)$ be the shifted kernel, and its corresponding reconstruction subspace be denoted by $\mathcal{W}_\tau$. Let Q_τ be the corresponding correction filter. Since $\widehat{w}_\tau(\omega) = e^{-j\tau\omega}\widehat{w}(\omega)$, thus the error kernel for the shifted interpolation becomes

$$\begin{aligned} E_\tau(\omega) = \; & 1 + |\widehat{q}_\tau(e^{j\omega})|^2 \sum_{n\in\mathbb{Z}} |\widehat{w}(\omega + 2\pi n)|^2 \\ & - 2\,\mathrm{Re}\left(e^{-j\tau\omega}\widehat{q}_\tau(e^{j\omega})\widehat{w}(\omega)\right) \end{aligned} \tag{17}$$

where $\widehat{q}_\tau$ is the frequency response of the filter Q_τ.

The dependency of E_τ on τ allows better interpolation with a suitable amount of shift. It was shown in [3] that in the limiting sampling case where $T\omega \to 0$, a 0.21-shift of the linear kernel can substantially improve the approximation quality.

Let $P_{\mathcal{W}_\tau}$ be the orthogonal projection on $\mathcal{W}_\tau$. From (4), we see that the error kernel of $P_{\mathcal{W}_\tau}$ is independent of the time shift. Hence

$$\begin{aligned} & \frac{1}{T}\int_0^T \|(I - P_{\mathcal{W}_\tau})x(\cdot - s)\|_2^2 \,\mathrm{d}s \\ & \quad = \frac{1}{T}\int_0^T \|(I - P_{\mathcal{W}})x(\cdot - s)\|_2^2 \mathrm{d}s \end{aligned}$$

for all $\tau \in \mathbb{R}$. This implies that shifting kernel does not affect the quality of the orthogonal projection as far as the average error is concerned. Moreover, shifting kernel can also preserve the approximation order of the interpolation process [21]. All these good properties suggest us to exploit this freedom of shifting kernel for a better interpolation toward orthogonal projection.

For the linear interpolation, for each $\tau \in [0, 1/2)$,[1] invoking (10) and (11), we obtain the correction filter

$$\widehat{q}_\tau(e^{j\omega}) = \frac{1}{1 - \tau + \tau e^{-j\omega}} \tag{18}$$

which renders the sampling to be interpolatory [3].

As a result, from (15) and (18), we have the corresponding error kernel [3]

$$\begin{aligned} E_\tau(\omega) = \; & 1 + \frac{2 + \cos\omega}{3|1 - \tau + \tau e^{-j\omega}|^2} \\ & - 2\,\mathrm{sinc}^2\left(\frac{\omega}{2\pi}\right)\,\mathrm{Re}\left(\frac{e^{-j\tau\omega}}{1 - \tau + \tau e^{-j\omega}}\right). \end{aligned} \tag{19}$$

To show the effects of shift on the interpolation quality, we plot in Fig. 1 the error kernel for four different values of τ ($\tau = 0.09, 1/8, 0.21, 0.30$). It is clear that while having little effect at low frequency up to $\pi/2$, shifting kernel w would have a significant impact on the approximation quality at high frequency (in particular around $\omega = \pi$). More significantly, the error kernel associate with $\tau = 0.09$ is seen to be very close to the benchmark kernel E_P. It is also pointed out that the optimal amount of shift of [3] (i.e., $\tau = 0.21$) appears to be not as good as the amount of shift $\tau = 0.09$. The latter would lead to better approximation at high frequency.

Fig. 1 clearly demonstrates that approximation quality can be further improved by optimizing over τ, and that the improvement can be significant for signals with major high frequency components.

[1]Note that if $\tau = 1/2$, then $q_\tau(e^{j\pi}) = \infty$ and thus $E_\tau(\pi)$ becomes extremely large.

IV. Optimal Shifts for Average Error

In this section, we determine the optimal amount of shift for two cases of input: the worst case and the average case (where the signal has an uniform distribution in frequency). We assume that x is band-limited by π/T to alleviate the aliasing effect. As a result, the optimization for the average error is dealt with by examining the restriction of E_τ on $[0, \pi]$, which is denoted by $E_\tau[0, \pi]$.

We now recall the following lemma [8], which helps to simplify the objective functions considered in the sequel.

Lemma 1: Let $g : \mathbb{R} \to \mathbb{R}$ be a bounded function. Then

$$\sup_{\|x\|_2 \le 1} \int_{\mathbb{R}} |g(t)|x^2(t)\mathrm{d}t = \max_{t\in\mathbb{R}} |g(t)|. \tag{20}$$

This equality still holds if the domain $\mathbb{R}$ is replaced with any interval (of nonzero length) in $\mathbb{R}$.

A. Optimal Shift in the Worst Case: $\min_\tau \|E_\tau[0, \pi]\|_\infty$

Now we aim to minimize the average error for all $x \in L^2$:

$$\min_{\tau\in[0,1/2)} J_\infty(\tau) \tag{21}$$

where the objective function J_∞ corresponds to the (squared) average error in the worst case:

$$\begin{aligned} J_\infty(\tau) = \; & \max_{\|x\|_2\le 1} \left\{e_x^2\right\} \\ = \; & \max_{\|x\|_2\le 1} \left\{\frac{1}{T}\int_0^T \|(I - WQ_\tau S^*)x(\cdot - s)\|_2^2 \,\mathrm{d}s\right\} \\ = \; & \max_{\|x\|_2\le 1} \int_{\mathbb{R}} E_\tau(\omega)\left|\widehat{x}\left(\frac{\omega}{T}\right)\right|^2 \frac{\mathrm{d}\omega}{2\pi T}. \end{aligned}$$

Under the π/T-band limited assumption, it becomes

$$J_\infty(\tau) = \max_{\|\widehat{x}\|_2\le 1} \int_{-\pi}^{\pi} E_\tau(\omega)\left|\widehat{x}\left(\frac{\omega}{T}\right)\right|^2 \frac{\mathrm{d}\omega}{2\pi T}.$$

In view of Lemma 1, we see that J_∞ is given by the maximum of E_τ in $[-\pi, \pi]$. Furthermore, since E_τ is an even function, we have

$$J_\infty(\tau) = \max_{\omega\in[0,\pi]} \left\{E_\tau(\omega)\right\}. \tag{22}$$

Therefore, we can find the optimal value of shift by optimizing the ∞-norm of $E_\tau[0, \pi]$.

B. Optimal Shift for Uniform Distribution: $\min_\tau \|E_\tau[0, \pi]\|_1$

The worst case is achieved by signals of very narrow band. It is thus very conservative for wide band inputs. When the frequency component is almost uniformly distributed up to the sampling frequency, it is more appropriate to consider the

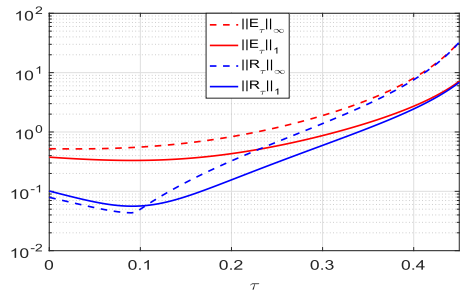

Fig. 3. The performance in terms of norms of the $[0,\pi]$-restriction of the error kernel E_τ and R_τ.

following optimization problem

$$\min_{\tau\in[0,1/2)} J_1(\tau) \tag{23}$$

where the objective function is the (expected) average of the error e_x^2 with respect to input x. When no *a priori* information on x other than the π/T-bandlimited assumption is available, it is reasonably to assume a uniform distribution for $\widehat{x}$. In addition, when the energy of x is unity, $|\widehat{x}(\omega/T)|^2$ is equal to T for $\omega\in[-\pi,\pi]$ or equal to zero elsewhere. Consequently, the objective function becomes

$$J_1(\tau)=2\int_0^\pi E_\tau(\omega)\,\frac{\mathrm{d}\omega}{2\pi}=\frac{1}{\pi}\|E_\tau[0,\pi]\|_1. \tag{24}$$

This implies that we can find the optimal value of shift by optimizing the 1-norm of $E_\tau[0,\pi]$.

C. Optimal Shifts for Linear Interpolation

In this section, we determine the optimal values of shift for the linear kernel.

1) Optimal shift in the worst case.

From the discussions in Section IV-A, the optimal value of shift is given as

$$\tau^*=\arg\min_{\tau\in[0,1/2)}\left\{\max_{\omega\in[0,\pi]}\{E_\tau(\omega)\}\right\} \tag{25}$$

where E_τ is given in (19). Equation (25) involves a simple two-variable minimax problem. By using the `fminimax` command of MATLAB, we obtain the optimal solution $\tau^*=0.0272$.

It is noted that for the linear kernel, E_τ is an monotonically increasing function of ω, thus,

$$\max_{\omega\in[0,\pi]}\{E_\tau(\omega)\}=E_\tau(\pi)=1+\frac{1}{3(1-2\tau)^2}-\frac{8\cos\pi\tau}{\pi^2(1-2\tau)}.$$

which can be shown to be concave in $\tau\in[0,1/2)$. Fig. 3 shows the plot of $\|E_\tau[0,\pi]\|_\infty$ in $\tau\in[0,0.45]$. It is seen that this ∞-norm has a very small variation in $\tau\in[0,0.10]$. This implies that any $\tau\in[0,0.10]$ would be near optimal as far as the worst case norm is concerned.

2) Optimal shift for uniform distribution.

From the discussions in Section IV-B, the optimal value of shift now is given as

$$\tau^*=\arg\min_{\tau\in[0,1/2)}\left\{2\int_0^\pi E_\tau(\omega)\,\frac{\mathrm{d}\omega}{2\pi}\right\} \tag{26}$$

where E_τ is given in (19). Solve this minimization problem by the `fminbnd` command of MATLAB, we obtain the optimal solution $\tau^*=0.0915$. The plot of $\|E_\tau\|_1$ for the linear kernel is also shown in Fig. 3 to show the effect of the shift.

To sum up, we see that the amount of shift $\tau=0.091$ ($\approx 1/11$ in the form of fraction) is optimal for J_1 and near optimal for J_∞. Since no further condition other than the band-limited or the uniform distribution assumption is used, we can conclude that generally speaking, when no further *a priori* information about x is available, the $1/11$-shifted linear kernel would be a near-optimal choice for a linear interpolation.

V. Shifting Kernel Toward Orthogonal Projection

Following the idea of minimax regret sampling but keeping the requirement of interpolatory sampling in Section III-B, we propose the following optimization problem

$$\min_{\tau\in[0,1/2)} J_{\mathrm{R}}(\tau) \tag{27}$$

where the objective function is

$$J_{\mathrm{R}}(\tau)=\max_{x\in\mathcal{X},\|x\|_{\mathcal{X}}\le 1}\left\{\frac{1}{T}\int_0^T\|(I-WQ_\tau S^*)x(\cdot-s)\|_2^2\,\mathrm{d}s - \frac{1}{T}\int_0^T\|(I-P_{\mathcal{W}})x(\cdot-s)\|_2^2\,\mathrm{d}s\right\} \tag{28}$$

where $(\mathcal{X},\|\cdot\|_{\mathcal{X}})$ is a Banach space which is introduced to incorporate *a priori* knowledge on input signals. Particular examples are specified later in this section.

The optimization is toward orthogonal projection in the spirit of minimax regret. Note that the use of filter Q_τ in (28) guarantees that the entire process is interpolatory for each τ. In essence, by subtracting the orthogonal projection error, the scheme effectively makes the process close to being orthogonal.

From (2), (3), (12), and (13), it follows that

$$J_{\mathrm{R}}(\tau)=\max_{x\in\mathcal{X},\ \|x\|_{\mathcal{X}}\le 1}\int_{\mathbb{R}}R_\tau(\omega)\left|\widehat{x}\left(\frac{\omega}{T}\right)\right|^2\frac{\mathrm{d}\omega}{2\pi T} \tag{29}$$

where

$$R_\tau(\omega)=E_\tau(\omega)-E_P(\omega) \tag{30}$$

is the error kernel for this minimax regret scheme, with E_τ and E_P being given in (17) and (4).

Let $\mathcal{X}=L^2$ with $\|\cdot\|_{\mathcal{X}}$ being the standard 2-norm. As in Section IV, objective function J_R can be similarly optimized in the worst case and for uniform distribution in terms of input $\widehat{x}$. And we can find optimal values of shift by minimizing the ∞-norm and 1-norm of the kernel $R_\tau[0,\pi]$, respectively.

When w is the linear kernel, we have from (4) and (19),

$$R_\tau(\omega)=\frac{2+\cos\omega}{3|1-\tau+\tau e^{-j\omega}|^2}+\frac{3\,\mathrm{sinc}^4\left(\frac{\omega}{2\pi}\right)}{2+\cos\omega} - 2\,\mathrm{sinc}^2\left(\frac{\omega}{2\pi}\right)\mathrm{Re}\left(\frac{e^{-j\tau\omega}}{1-\tau+\tau e^{-j\omega}}\right). \tag{31}$$

Again, using the `fminimax` and `fminbnd` commands of the MATLAB, we obtain the optimal values of shift for the ∞-norm

and the 1-norm of the $[0,\pi]$-restriction of kernel R_τ. The values are $\tau = 0.0910$ and $\tau = 0.0915$, respectively, both of which can be approximated by the fraction $1/11$. See Fig. 3 for plots of both norms as functions of τ.

When we have some *a priori* knowledge on the input signal, better shifting is possible for the minimax regret sampling. Based on properties of the input signals, we now consider three different cases: 1) they belong to some T-shiftable subspace, 2) they belong to some Sobolev subspace, and 3) they are from natural images.[2]

A. T-Shiftable Subspaces

Assume that Banach space $\mathcal{X}$ is the T-shiftable subspace of L^2 with generating kernel v, that is,

$$x \in \mathcal{V} = \left\{ x(t) = \sum_{n\in\mathbb{Z}} a_n v\left(\frac{t}{T} - n\right), \{a_n\} \in \ell^2 \right\}. \quad (32)$$

We assume that $\{v(\frac{\cdot}{T} - n)\}_{n\in\mathbb{Z}}$ constitutes a frame of $\mathcal{V}$.

If $x \in \mathcal{V}$, then from (32), we can rewrite

$$\widehat{x}\left(\frac{\omega}{T}\right) = T\widehat{a}(e^{j\omega})\widehat{v}(\omega) = a_0(e^{j\omega})\widehat{v}_0(\omega)$$

where

$$\widehat{v}_0(\omega) = \begin{cases} \frac{\widehat{v}(\omega)}{\sqrt{A_V(\omega)}}, & \text{if } A_V(\omega) \neq 0 \\ 0, & \text{otherwise} \end{cases}$$

is the 1-tight frame function for $\mathcal{V}$ with $A_V(\omega) = \sum_{n\in\mathbb{Z}} |\widehat{v}(\omega + 2\pi n)|^2$, and $\widehat{a}_0(e^{j\omega}) = T\widehat{a}(e^{j\omega})\sqrt{A_V(\omega)}$ being the corresponding coefficients [10], [28]. Moreover, in view of the norm-preserving property of 1-tight frames [28], from (29) we have

$$\begin{aligned} J_R(\tau) &= \max_{\|a_0\|_2^2 = T} \int_{\mathbb{R}} R_\tau(\omega) |\widehat{a}_0(e^{j\omega})|^2 |\widehat{v}_0(\omega)|^2 \frac{\mathrm{d}\omega}{2\pi T} \\ &= \max_{\|a_0\|_2^2 = T} \int_{-\pi}^{\pi} |\widehat{a}_0(e^{j\omega})|^2 \sum_{n\in\mathbb{Z}} R_\tau(\omega + 2\pi n) \\ &\quad \times |\widehat{v}_0(\omega + 2\pi n)|^2 \frac{\mathrm{d}\omega}{2\pi T} \\ &= \max_{\omega\in[-\pi,\pi]} \left\{ \sum_{n\in\mathbb{Z}} R_\tau(\omega + 2\pi n) \, |\widehat{v}_0(\omega + 2\pi n)|^2 \right\} \\ &= \max_{\omega\in[0,\pi]} \left\{ \sum_{n\in\mathbb{Z}} R_\tau(\omega + 2\pi n) |\widehat{v}_0(\omega + 2\pi n)|^2 \right\} \quad (33) \end{aligned}$$

where the second to last step is from Lemma 1, and the last step is from the symmetry of the magnitude spectra of real signals.

As a result, the optimal value of shift can be obtained by minimizing J_R in (33). And it can be solved by using the `fminimax` command.

[2]Note that image interpolation can be performed in a separable manner, i.e., by successive interpolation on rows and columns.

For the linear interpolation kernel, from (31) it follows that

$$\begin{aligned} R_\tau(\omega + 2\pi n) &= \frac{2 + \cos\omega}{3|1 - \tau + \tau e^{-j\omega}|^2} + \frac{3\,\mathrm{sinc}^4\left(\frac{\omega}{2\pi} + n\right)}{2 + \cos\omega} \\ &\quad - 2\,\mathrm{sinc}^2\left(\frac{\omega}{2\pi} + n\right) \mathrm{Re}\left[\frac{e^{-j\tau(\omega + 2\pi n)}}{1 - \tau + \tau e^{-j\omega}}\right]. \end{aligned}$$

Moreover, if the generating kernel is the B-spline of order m [22], i.e., $v(t) = \beta^m(t)$, then $\widehat{v}(\omega) = \mathrm{sinc}^{m+1}(\omega/(2\pi))$. Therefore,

$$|\widehat{v}_0(\omega + 2\pi n)|^2 = \frac{\mathrm{sinc}^{2(m+1)}\left(\frac{\omega}{2\pi} + n\right)}{\sum_{k\in\mathbb{Z}} \mathrm{sinc}^{2(m+1)}\left(\frac{\omega}{2\pi} + k\right)}.$$

Consequently, we have

$$\begin{aligned} \sum_{n\in\mathbb{Z}} R_\tau(\omega + 2\pi n)|\widehat{v}_0(\omega + 2\pi n)|^2 &= \frac{2 + \cos\omega}{3|1 - \tau + \tau e^{-j\omega}|^2} \\ &\quad + 2\mathrm{Re}\left[\frac{\sum_{k=-m-1}^{m+2} \beta^{2m+3}(k - \tau) e^{-jk\omega}}{1 - \tau + \tau e^{j\omega}}\right] \\ &\quad + \frac{\beta^{2m+5}(0) + 2\sum_{k=1}^{m+2} \beta^{2m+5}(k)\cos k\omega}{2 + \cos\omega}. \end{aligned}$$

For $m = 1, 2, 3$ and 10, the optimal amount of shifts are found to be $\tau = 0.0699$, 0.0790, 0.0823, and 0.0906, respectively. The corresponding functions J_R are plotted in Fig. 4(a).

Note that if $m \to \infty$, then $\widehat{v}_0(\omega)$ approaches to the indicator function $\mathbf{1}_{[-\pi,\pi]}(\omega)$ [2]. The objective function then simplifies, in view of (33), to

$$J_R(\tau) = \max_{\omega\in[0,\pi]} R_\tau(\omega).$$

Therefore, the optimal amount of shift is again $\tau = 0.0910$.

B. Sobolev Subspaces

Now assume that the input signals are in the Sobolev space of order r [9], that is,

$$\mathcal{X} = W^r = \{x(t) : \|x\|_{\mathrm{sob}} < \infty\}$$

with the Sobolev norm being defined as

$$\|x\|_{\mathrm{sob}} = \left(\int_{\mathbb{R}} (1 + \omega^2)^r \left| \widehat{x}\left(\frac{\omega}{T}\right) \right|^2 \frac{\mathrm{d}\omega}{2\pi T} \right)^{\frac{1}{2}}.$$

The minimax regret objective function in (29) can be simplified as

$$\begin{aligned} J_{\mathrm{R}}(\tau) &= \max_{x\in W^r,\, \|x\|_{\mathrm{sob}} \leq 1} \int_{\mathbb{R}} R_\tau(\omega) \left| \widehat{x}\left(\frac{\omega}{T}\right) \right|^2 \frac{\mathrm{d}\omega}{2\pi T} \\ &= \max_{x\in W^r,\, \|x\|_{\mathrm{sob}} \leq 1} \int_{\mathbb{R}} \left[\frac{R_\tau(\omega)}{(1+\omega^2)^r}\right] \left[(1+\omega^2)^r \left| \widehat{x}\left(\frac{\omega}{T}\right) \right|^2 \right] \\ &\quad \times \frac{\mathrm{d}\omega}{2\pi T} \\ &= \max_{\|y\|_2 \leq 1} \int_{\mathbb{R}} \left[\frac{R_\tau(\omega)}{(1+\omega^2)^r}\right] \left| \widehat{y}\left(\frac{\omega}{T}\right) \right|^2 \frac{\mathrm{d}\omega}{2\pi T} \\ &= \max_{\omega\in[0,\infty)} \frac{R_\tau(\omega)}{(1+\omega^2)^r} \end{aligned}$$

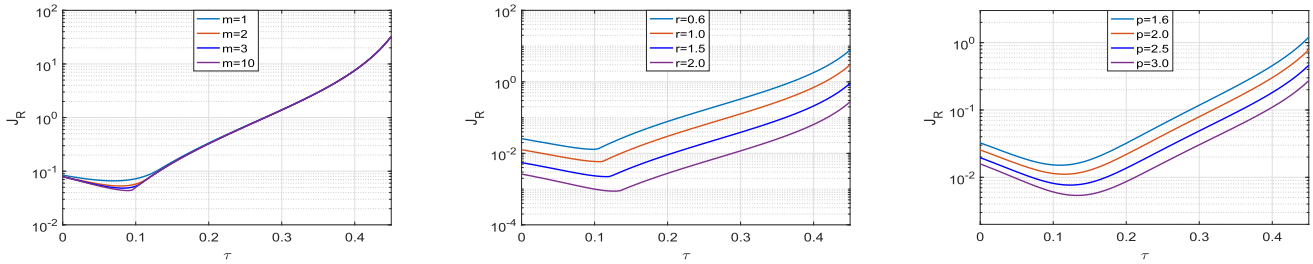

(a) (b) (c)

Fig. 4. Minimax regret error function J_R for various input signals: (a) Shiftable subspaces of B-spline of order m, (b) Sobolev subspace of order r, and (c) Natural signals with power p.

where the last step is from Lemma 1 and symmetry of R_τ.

For π/T-bandlimited input, it becomes

$$J_{\mathrm{R}}(\tau) = \max_{\omega\in[0,\pi]} \frac{R_\tau(\omega)}{(1+\omega^2)^r}. \tag{34}$$

Again, the optimal value of shift can be obtained by solving the minimax problem involving J_R in (34). For orders $r = 0.6, 1.0, 1.5,$ and 2.0, the optimal values of the shifts are found, using the `fminimax` command, to be $\tau = 0.1002, 0.1069, 0.1164,$ and 0.1269, respectively. Fig. 4(b) shows the effect of τ on the maximum error J_R for these orders.

C. Natural Signals

Now we consider signals arisen from natural images, It is acknowledged that these signals tend to exhibit (negative) power spectrum [13]. That is,

$$|\widehat{x}(\omega)|^2 \approx \frac{c}{|T\omega|^p}\mathbf{1}_{[-\pi,\pi]}(T\omega)$$

for some scalar $c \geq 0$ and parameter $p > 0$ which varies from 1.6 to 3.0. Accordingly, for each p, the minimax regret sampling can be improved toward orthogonal projection by minimizing

$$J_{\mathrm{R}}(\tau) = \int_{-\pi}^{\pi} \frac{R_\tau(\omega)}{|\omega|^p}\frac{\mathrm{d}\omega}{2\pi} = 2\int_0^{\pi} \frac{R_\tau(\omega)}{\omega^p}\frac{\mathrm{d}\omega}{2\pi}. \tag{35}$$

Now consider the linear interpolation kernel, for which the expression of R_τ is given in (31). Let $p = 1.6, 2.0, 2.5,$ and 3.0. Fig. 4(c) shows the corresponding plots of J_R. Using the `fminbnd` command, we obtain the optimal values of shift $\tau = 0.1092, 0.1150, 0.1181,$ and 0.1737, respectively.

VI. Experiments

This sections evaluates the performance of the shifted linear interpolations through some examples. We consider five types of input: 1) an Gaussian signal, 2) an ECG signal, 3) a speech signal, 4) a 2-dimensional signal, and 5) three natural images.[3]

A. Practical Issues

Fig. 5 shows the block diagram of the τ-shifted linear interpolation. We now discuss the relevant issue of computational load. Assume that we have N samples of signal x available. Let the number of points at which the reconstruction needs to be performed be M. First, as in the standard case, the reconstruction operator W_τ needs $2M$ multiplications and M additions in view of the short-support of the linear kernel β_τ. The only extra computation introduced by shift is due to the correction filter Q of (18), which amounts to $2N$ multiplications and N additions if Q is implemented recursively:

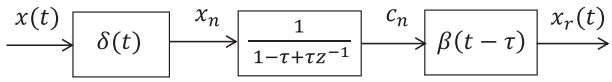

Fig. 5. The block diagram of the τ-shifted linear interpolation.

$$c_n = -\frac{\tau}{1-\tau}c_{n-1} + \frac{1}{1-\tau}x_n. \tag{36}$$

Note that in practice, N is usually much smaller than M. Therefore, the shifted interpolation enjoys a computational load which is comparable to that of the standard linear interpolation and is much smaller than those of higher order interpolations. We refer [3] for more details on the computational cost.

Assume that we want to re-sample signal x at $kT + \mu T$ from $\{x_n\}_{n\in\mathbb{Z}}$ for some $k \in \mathbb{Z}$ and $0 < \mu < 1$. With the τ-shifted linear kernel,

$$\begin{aligned} x(kT+\mu T) &= \sum_{n\in\mathbb{Z}} c_n \beta_\tau\left(\frac{kT+\mu T}{T} - n\right) \\ &= \sum_{n\in\mathbb{Z}} c_n \beta(k+\mu-\tau-n). \end{aligned}$$

Since $\beta(0) = 1$, $\beta(t) = 0$ for $|t| > 1$, and $|\mu - \tau| < 1$, thus

$$x(kT+\mu T) = \begin{cases} c_{k-1}\beta(\mu-\tau+1) + c_k\beta(\mu-\tau), & \mu < \tau \\ c_k & \mu = \tau \\ c_k\beta(\mu-\tau) + c_{k+1}\beta(\mu-\tau-1), & \mu > \tau. \end{cases}$$

We can see from (36) that when $\mu \leq \tau$, x_{k+1} is not used in the re-sampling. As a result, the τ-shifted linear interpolation is less likely to yield small approximation error at $kT + \mu T$. This implies that for a given re-sampling step, the amount of a kernel shift that is to be used should be smaller than the size of the step in order to achieve better approximation. Illustrative examples will be provided in Section VI-F.

[3]Some relevant Matlab files are available at: https://www.researchgate.net/profile/Runyi_Yu.

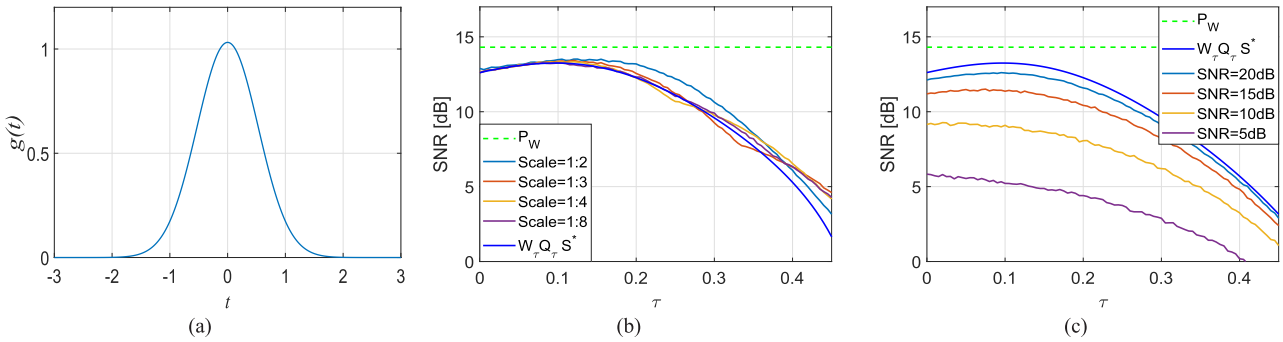

Fig. 6. The performance comparison of the τ-shifted linear interpolation for (a) a Gaussian signal (b) under various scales and (c) under different noise levels.

Following our discussions in Section V and many experiments, we recommend a common value of $\tau = 1/8 = 0.125$ for the shifted linear interpolation when processing natural signals/images. The fraction of $1/8$ is very close to the average (which is equal to 0.1208) of the optimal values obtained in Sections V-B and V-C. Also, the dyadic power expression $1/8 = 1/2^3$ would have some advantages in practical implementation [3], [27].

B. Gaussian Signal Interpolation

Let $T = 1$ and the input be the Gaussian signal

$$g(t) = 1/(2\pi\alpha)^{1/4} e^{-t^2/(4\alpha)} \tag{37}$$

which is plotted in Fig. 6(a), where $\alpha = 2\ln(2)/\pi^2$. Note that g has a unity energy (thus, $\|g\|_2 = 1$) and half-power frequency of $\pi/2$, and that 98.0% of its energy lies in the Nyquist band.

For each $\tau \in [0, 0.45]$, the Gaussian g is reconstructed to become g_r as in Fig. 2 using the τ-shifted linear kernel. We then compute the signal-to-noise ratio (SNR) for each reconstruction by

$$\text{SNR} = 10\log \frac{\|g\|_2^2}{\|g - g_r\|_2^2} = -20\log \|g - g_r\|_2.$$

The result is presented in Fig. 6(b) (the blue line) as indicated by legend $W_\tau Q_\tau S^*$. For comparison, Fig. 6(b) also shows (the dashed line) the error (SNR $= 14.32$ dB) of the orthogonal projection P_W. It is clear that the τ-shifted linear interpolation outperforms the standard interpolation (with SNR $= 12.60$ dB) for $\tau < 0.17$. The highest SNR $= 13.28$ dB is yielded if $\tau = 0.09$. Note that when $\tau = 0.21$, the SNR is only 12.08 dB.

Next, assume that only the sample S^*g is available. High-resolution signals can be generated through interpolation by determining the values of g between the sampling instants at fine grids. For scale $1 : N$, we can insert $N - 1$ samples (equally spaced in time) between the original samples. Fig. 6(b) show the average squared errors for $N = 2, 3, 4, 8$ for the Gaussian signal g, where the average is calculated over 5000 random input shifts that are uniformly generated in $[0, 1]$. We see that the $1/8$-shifted interpolation yield SNRs that are greater than those by the standard and 0.21-shifted linear interpolations. Further, the SNR from the $1/8$-shift is also very close to the maximum SNR achievable.

Finally, we compare the linear interpolation kernels under noise measurement. For this purpose, signal g is contaminated with independent and identically distributed Gaussian noise of zero mean. We then evaluate the reconstruction performance under the noise level with SNR $= 20, 15, 10, 5$ dB. Fig. 6(c) presents the SNRs of the reconstructions. As expected, the SNR of the reconstruction decreases as the noise level increases. Nevertheless, the $1/8$-shifted interpolation would give the largest SNR in case of strong signals (with SNR > 15 dB of noise level). For the weak signal case (with SNR < 10 dB of noise level), on the other hand, the standard interpolation results in the maximum SNR because of the effect of the noise in relation to the spectrum of g.

C. ECG Signal Interpolation

We download an ECG signal from PhysioNet [12]. It is the 10-second version of record 1672.dat file of the ECG1 signal from the MIT-BIH Normal Sinus Rhythm Database. The signal was obtained with a sampling rate of $f_s = 128$ Hz.

For the purpose of performance evaluation, we down-sample this ECG signal by a factor of 2. This leads to a reduction of Nyquist frequency by $1/2$ and the new Nyquist band becomes $[0, 64]$ Hz. Nevertheless, since 98.3% of the energy of the ECG signal is in the new band, our discussions and results of shifted linear interpolations are still relevant. Let us now apply the standard and the shifted linear interpolations (with $\tau = 1/8$ and 0.21) to obtain approximates of the original. The results are shown in Fig. 7. Note that while the 0.21-shifted interpolation improves the standard interpolation by 0.54 dB, the $1/8$-shifted interpolation achieves a better improvement of 1.46 dB. The improvement is also evident from the three error curves shown at lower part of Fig. 7. In terms of the maximal error, the improvements are 1.5% and 12.8%, respectively.

D. Speech Signal Interpolation

We start with a speech record of 70 milliseconds (of the first author) at a sampling rate of 4.41 kHz (the Nyquist frequency of speech signals). This signal is down-sampled by a factor of 2. Similar to the case of ECG signal, this speech signal has 99.9% of its energy in the new Nyquist band $[0, 2.205]$ kHz. We now apply the standard and the shifted linear interpolations (with $\tau = 1/8$ and 0.21) to the down-sampled signal.

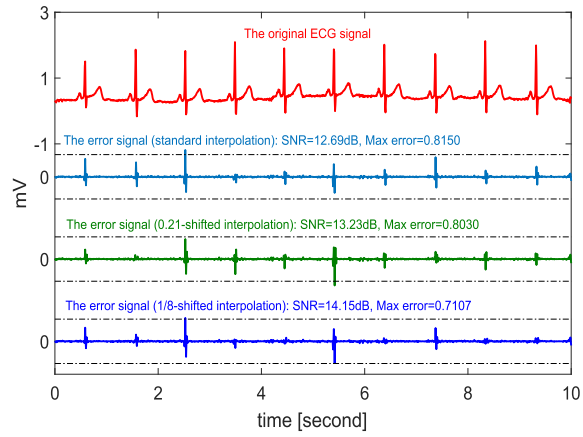

Fig. 7. An ECG signal and comparison of the interpolation error signals.

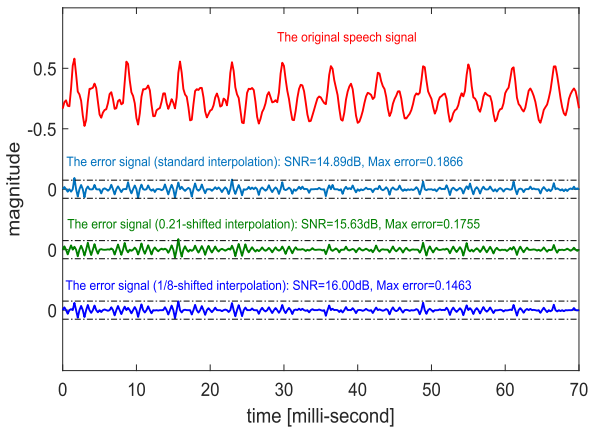

Fig. 8. A speech signal and comparison of the interpolation error signals.

The resulting signals are compared with the original record, and are shown in Fig. 8. We see that while the 0.21-shifted interpolation improves the standard interpolation by 0.74 dB, the $1/8$-shifted interpolation achieves a better improvement of 1.11 dB. In terms of the maximal error, the $1/8$-shifted interpolation results in a very good reduction of 21.6%, compared with a value of 5.9% for the 0.21-shifted interpolation.

E. Natural Image Zooming

We now apply the shifted linear interpolation to two natural images: the House and the Cameraman of 512×512 shown in Figs. 9 and 10, respectively.[4] The interpolation is carried out by successive interpolations on rows and columns.

As to the ECG signal in Section VI-C, each image is first zoomed-out (down-sampled by 2). We then perform the shifted linear interpolation for the down-sampled image. Determining the pixel values at the middle points results in a zoomed-in image, which is then used to compare with the original image. We also perform the standard and the cubic interpolations. The latter is used since it 'is known to represent the best trade-off between performances and computational complexity' [1]. The quantitative comparison in terms of the SNR, the peak signal-to-noise ratio (PSNR),[5], and the structural similarity index (SSIM) [29] of the results are given in Table I.

The comparison show that the $1/8$-shifted linear interpolation significantly outperforms the standard linear interpolation (by more than 2 dB in SNR and PSNR for the house, and more than 1 dB for the Cameraman). While compared unfavourably to the cubic interpolation as expected, the $1/8$-shifted interpolation is closer to it than to the standard linear interpolation. Note that the 0.21-shifted linear interpolation provides lesser improvement compared with the $1/8$-shift. Furthermore, a close inspection of Figs. 9 and 10 also show that the images obtained using the $1/8$ shift are perceptually less blurred and sharper around edges (for example, the roof and the window in Fig. 9, and the hairs and shoulder in Fig. 10) when compared with those from other linear interpolations.

F. Successive 2-dimensional Rotations

We now consider a 2-dimensional separable continuous-time signal

$$x(t, s) = g(t)\,\mathrm{sinc}\,(s) \tag{38}$$

where $g(t)$ is the Gaussian signal given in (37) and the sinc function is $\mathrm{sinc}\,(s) = \sin(\pi s)/(\pi s)$. As a synthetic image, $x(t, s)$ is shown in Fig. 11(a).

We now perform successive rotations of $x(t, s)$ using the three linear kernels. Let the rotation angle be $\theta \in \{5\pi k/180 \text{ rad} : k = 1, 2, \ldots, 17\} = \{(5k)^\circ : k = 1, 2, \ldots, 17\}$. For each such angle, the number of rotations is selected to be $\lceil 90^\circ/\theta \rceil$. And the SNR of the resulted signal is shown in Fig. 11(c). Note that the $1/8$-shifted interpolation outperforms both the standard and the 0.21-shifted interpolations for rotation angle $\theta \geq 20^\circ$. For small rotation angles ($\theta < 20^\circ$), the standard linear kernel gives the highest SNR values, which is consistent to our discussions in Section VI-A.

Next, we turn to successive rotations of digital images. Now, the angle and number of rotations need to be properly selected so that an accurate comparison to the ground truth is possible. Let the number of rotations be $n = 2, 3, \ldots, 18$, each associated with an angle of $90^\circ/n$. Then the SNR of the resultant images can be calculated. Fig. 11(d) shows the results for the Mandrill image of 512×512 of Fig. 11(b). Again, we see that the $1/8$-shifted interpolation outperforms both the standard and the 0.21-shifted interpolations for big rotation angle (larger than 8°); And for the small angles, the standard interpolation yields the best result. We have the same observation for other test images of the same size, including the Lena, the Pepper, and the Walkbridge.

We conclude that the $1/8$-shifted linear interpolation improves the image rotation results for 2-dimensional signals/images having significant high frequency contents under large rotation angles. However, the situation for image rotation is generally rather complicated, Not only is the performance

[4]All images tested in this paper are downloaded from http://www.imageprocessingplace.com.

[5]The PSNR is defined (in dB) as $\mathrm{PSNR} = 10\log(|\max\{|x(\cdot)|\}|^2 / e_x^2) = 20\log 255 - 20\log e_x$.

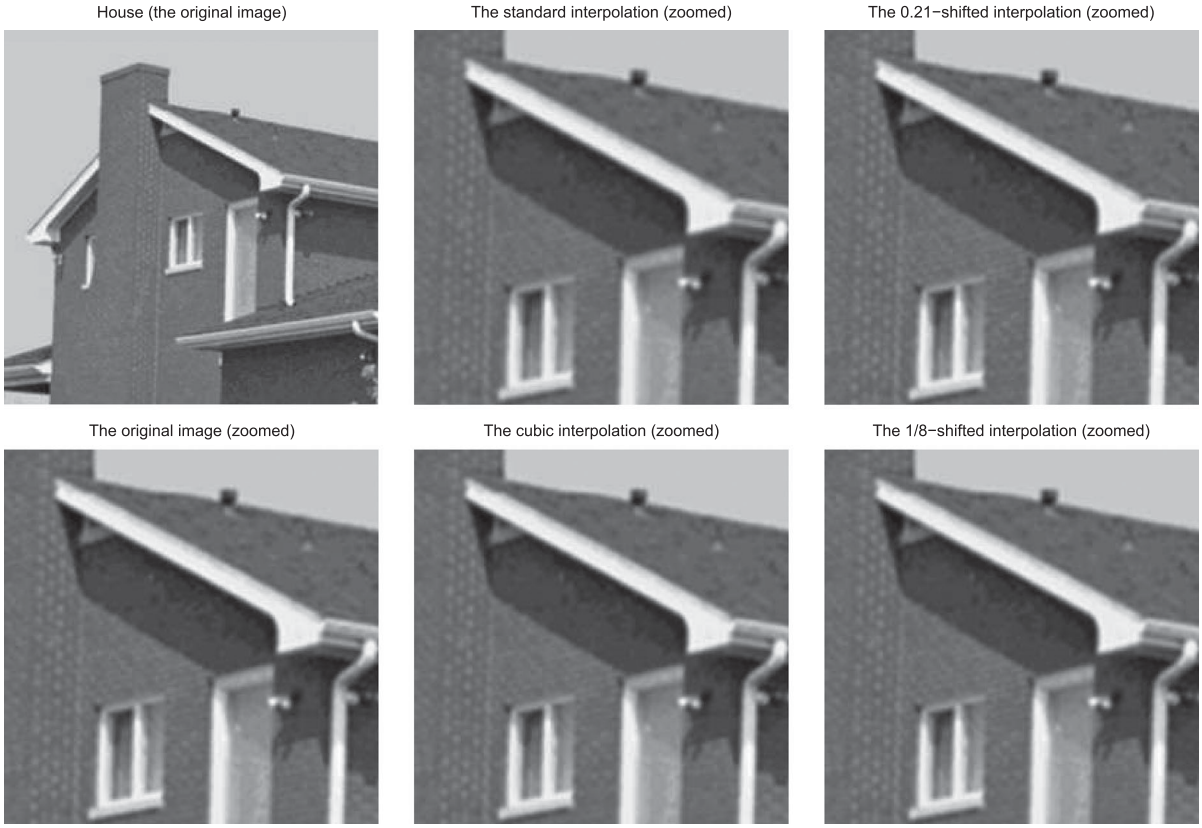

Fig. 9. Image interpolations of the House.

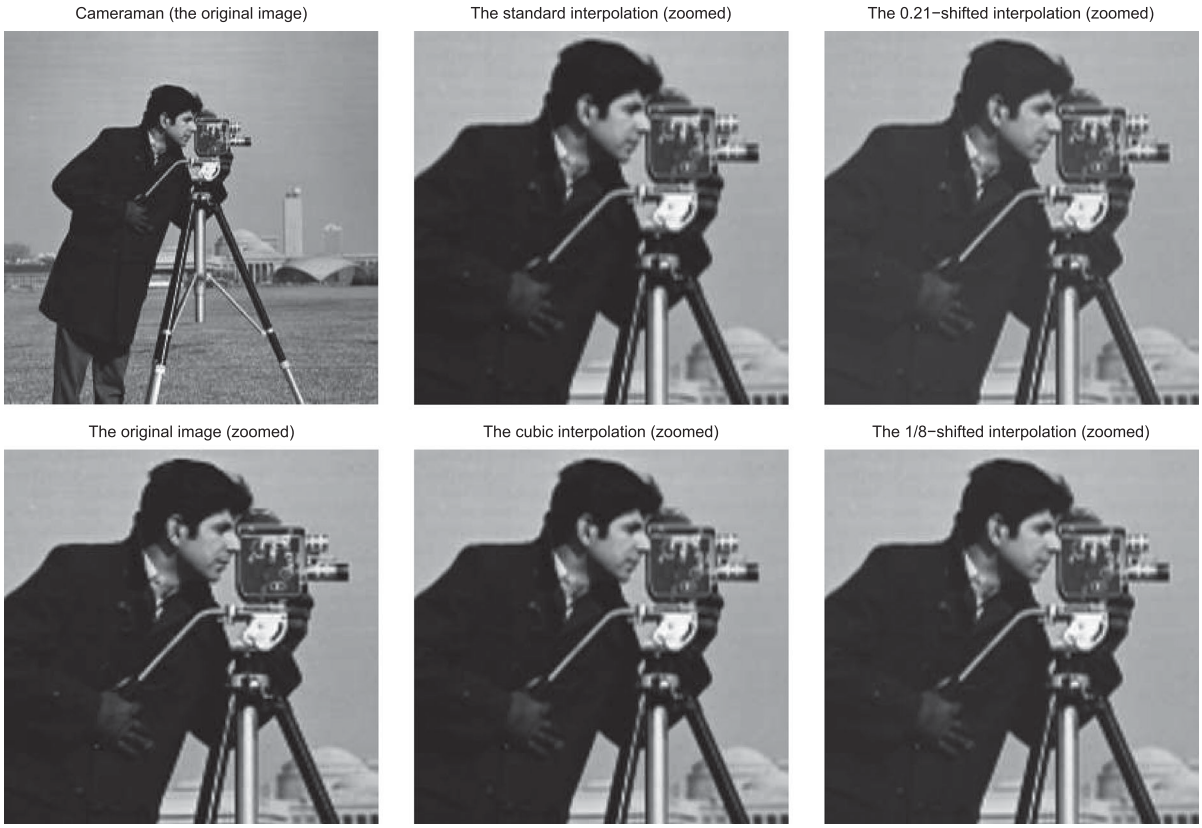

Fig. 10. Image interpolations of the Cameraman.

TABLE I
THE PERFORMANCE OF THE INTERPOLATIONS

Interpolation method	SNR (dB)		PSNR (dB)		SSIM	
	House	Cameraman	House	Cameraman	House	Cameraman
the standard linear	39.91	30.62	44.64	36.24	0.9970	0.9894
the 0.21-shifted	40.87	30.80	45.60	36.42	0.9976	0.9917
the $1/8$-shifted	41.92	31.69	46.65	37.32	0.9980	0.9919
the cubic	43.03	32.49	47.76	38.12	0.9982	0.9921

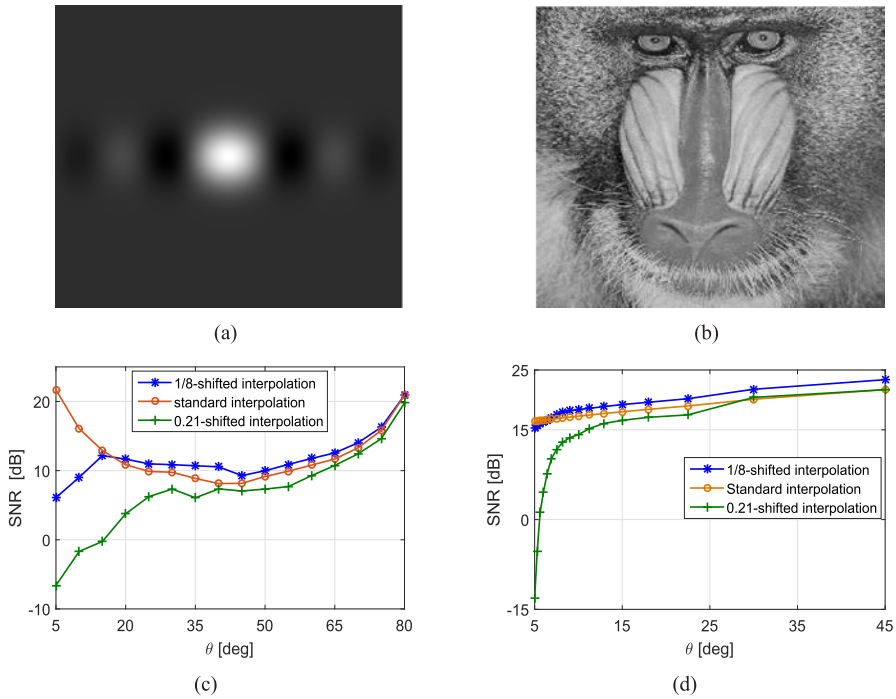

Fig. 11. The performance comparison of three linear interpolations under successive rotations: a synthetic signal (a) and the respective SNR values (c); and a Mandrill image (b) and the respective SNR values (d).

dependent on the amount of the kernel shift, it is also closely related to the angle of rotations and the number of rotations. It is very complicated also because for each angle the amounts of (horizontal and vertical) offsets vary from position to position. And in the case of small rotation angles, such offsets can be much smaller than the kernel shift. Accordingly, it would be very beneficial if the shift is adjusted adaptively according to the given image as well as the position of the pixel that is being rotated. For further performance improvement of image rotation, it would be intriguing to have a separate study of kernels in polar form instead of the separable form.

VII. CONCLUSIONS

In this paper we proposed a new notion of kernel shifting that renders the resulted shifted interpolation to approach the orthogonal projection in the minimax regret sense. In this method, we took the average approximation error as the quality measure and obtained the optimal amount of the shift so that for each relevant input, the reconstruction from the shifted interpolation is the closest to the corresponding orthogonal projection. In addition, the shifted interpolation also possesses the good property of being interpolatory (thus consistent) through the use of correction filter.

For the linear interpolation, we recommend two values of shift: $\tau = 1/8$ for smooth signals and natural images, and a smaller value $\tau = 1/11$ for arbitrary signals for which no *a priori* knowledge is available. We showed that the corresponding shifted interpolation significantly outperform the standard linear interpolation. Further improvements would be possible when the shifted interpolation is carried out with edge-orientation taken into account since then the high frequency component would be more prevailing. In addition, it would be practically advantageous to develop an adaptive mechanism that adjusts the amount of kernel shift depending on the given signal.

We anticipate that benefits would also be possible for generalized sampling-reconstruction processes through shifting kernel, especially when the reconstruction kernel is asymmetric or is of short support, as is the case of most orthogonal scaling and wavelet functions or many short window functions. Note that the benefit would be marginal if the process is already close to the orthogonal projection, such as the case for higher order-spline interpolation [23], [24].

Furthermore, the framework in this paper can be extended to high dimensional spaces. In this case, additional advantages to the reconstruction may be possible if some format of shifting not in the separable form is used. For this purpose, a new formulation and derivation of the average approximation error would be required.

REFERENCES

[1] B. Aiazzi, S. Baronti, M. Selva, and L. Alparone, "Bi-cubic interpolation for shift-free pan-sharpening," *ISPRS J. Photogramm. Remote Sens.*, vol. 86, pp. 65–76, Dec. 2013.

[2] A. Aldroubi, M. Unser, and M. Eden, "Cardinal spline filters: Stability and convergence to the ideal sinc interpolator," *Signal Process.*, vol. 28, pp. 127–138, Aug. 1992.

[3] T. Blu, P. Thevenaz, and M. Unser, "Linear interpolation revitalized," *IEEE Trans. Image Process.*, vol. 13, no. 5, pp. 710–719, May 2004.

[4] T. Blu and M. Unser, "Quantitative Fourier analysis of approximation techniques: Part I – Interpolators and projectors," *IEEE Trans. Signal Process.*, vol. 47, no. 10, pp. 2783–2795, Oct. 1999.

[5] Y. Cha and S. Kim, "The error-amended sharp edge (EASE) scheme for image zooming," *IEEE Trans. Image Process.*, vol. 16, no. 6, pp. 1496–1505, Jun. 2007.

[6] J. Choi and M. Kim, "Super-interpolation with edge-orientation-based mapping kernels for low complex 2x upscaling," *IEEE Trans. Image Process.*, vol. 25, no. 1, pp. 469–483, Jan. 2016.

[7] K. K. Delibasis and A. Kechriniotis, "A new formula for bivariate Hermite interpolation on variable step grids and its application to image interpolation," *IEEE Trans. Image Process.*, vol. 23, no. 7, pp. 2892–2904, Jul. 2014.

[8] J. Doyle, B. Francis, and A. Tannenbaum, *Feedback Control Theory*. New York, NY, USA: Macmillan, 1990.

[9] G. Dvorkind, H. Kirshner, Y. C. Eldar, and M. Porat, "Minimax approximation of representation coefficients from generalized samples," *IEEE Trans. Signal Process.*, vol. 55, no. 9, pp. 4430–4443, Aug. 2007.

[10] Y. C. Eldar and T. Dvorkind, "A minimum squared-error framework for generalized sampling," *IEEE Trans. Signal Process.*, vol. 54, no. 6, pp. 2155–2167, Jun. 2006.

[11] Y. C. Eldar and T. Michaeli, "Beyond bandlimited sampling," *IEEE Signal Process. Mag.*, vol. 26, no. 3, pp. 48–68, May 2009.

[12] A. L. Goldberger *et al.*, "PhysioBank, physioToolkit, and physioNet: Components of a new research resource for complex physiologic signals," *Circulation*, vol. 101, Jun. 2000.

[13] W. H. Hsiao and R. P. Millane, "Effects of occlusion, edges, and scaling on the power spectra of natural images, *J. Opt. Soc. Amer. A*, vol. 22, pp. 1789–1797, 2005.

[14] C. Lee, M. Eden, and M. Unser, "High-quality image resizing using oblique projection operators," *IEEE Trans. Image Process.*, vol. 7, no. 7, pp. 679–692, Sep. 2001.

[15] T. M. Lehmann, C. Gönner, and K. Spitzer, "Survey: Interpolation methods in medical image processing," *IEEE Trans. Med. Imag.*, vol. 18, no. 11, pp. 1049–1075, Nov. 1999.

[16] A. Muñoz, T. Blu, and M. Unser, "Least-square image resizing using finite differences," *IEEE Trans. Image Process.*, vol. 10, no. 9, pp. 1365–1378, Sep. 2001.

[17] G. Plonka, "Optimal shift parameters for periodic spline interpolation," *Numer. Algorithms*, vol. 6, pp. 481–510, Mar. 1994.

[18] B. Sadeghi and R. Yu, "Shift-variance and cyclostationarity of linear periodically shift-variant systems," presented at the 10th Int. Conf. Sampling Process. Theory Appl., Bremen, Jul. 2013.

[19] B. Sadeghi and R. Yu, "Shift-variance and nonstationarity of linear periodically shift-variant systems and applications to Generalized sampling and reconstruction processes," *IEEE Trans. Signal Process.*, vol. 64, no. 6, pp. 1493–1506, Mar. 2016.

[20] L. Sacht and D. Nehab, "Optimized quasi-interpolation for image reconstruction," *IEEE Trans. Image Process.*, vol. 24, no. 12, pp. 5249–5259, Dec. 2015.

[21] P. Thévenaz, T. Blu, and M. Unser, "Interpolation revisited," *IEEE Trans. Med. Imag.*, vol. 19, no. 7, pp. 739–758, Jul. 2000.

[22] M. Unser, "Sampling – 50 years after Shannon," *Proc. IEEE*, vol. 88, no. 4, pp. 569–587, Apr. 2000.

[23] M. Unser, "B splines – A perfect fit for signal and image processing," *IEEE Signal Process. Mag.*, vol. 16, no. 6, pp. 22–38, Nov. 1999.

[24] M. Unser, "Ten good reasons for using spline wavelets," *Proc. SPIE Wavelets Appl. Signal Image Process.*, vol. 3169, pp. 422–431, 1997.

[25] M. Unser and A. Aldroubi, "A general sampling theory for nonideal acquisition devices," *IEEE Trans. Signal Process.*, vol. 42, no. 11, pp. 2915–2925, Nov. 1994.

[26] M. Unser, A. Aldroubi, and M. Eden, "B-Spline signal processing: Part I – Theory," *IEEE Trans. Signal Process.*, vol. 41, no. 2, pp. 821–833, Feb. 1993.

[27] M. Unser, A. Aldroubi, and M. Eden, "B-Spline signal processing. II. Efficient design and applications," *IEEE Trans. Signal Process.*, vol. 41, no. 2, pp. 834–848, Feb. 1993.

[28] M. Vetterli, J. Kovacevic, and V. K. Goyal, *Foundation of Signal Processing*. Cambridge, U.K.: Cambridge Univ. Press, 2014.

[29] Z. Wang, A. C. Bovik, H. R. Sheikh, and E. P. Simoncelli, "Image quality assessment: From error visibility to structural similarity," *IEEE Trans. Image Process.*, vol. 13, no. 4, pp. 600–612, Apr. 2004.

[30] R. Yu, "Shift-variance analysis of generalized sampling processes," *IEEE Trans. Signal Process.*, vol. 60, no. 6, pp. 2840–2850, Jun. 2012.

Bashir Sadeghi (S'12) received the B.S. degree in electrical and computer engineering from Noshirvani University of Technology, Babol, Iran, and the M.S. degree in electrical and electronic engineering from Eastern Mediterranean University, Gazimagusa, North Cyprus. He is currently working toward the Ph.D. degree in the Department of Electrical and Electronic Engineering, Eastern Mediterranean University. His research interests are in the general areas of signal processing and machine learning, especially generalized sampling and reconstruction processes, computer vision, wavelet analysis, and statistical signal processing.

Runyi Yu (M'95–SM'99) received the Ph.D. degree in automatic control from Beijing University of Aeronautics and Astronautics, Beijing, China.

He is a Professor in the Department of Electrical and Electronic Engineering, Eastern Mediterranean University, Gazimagusa, North Cyprus. He has authored or coauthored more than 60 journal or conference publications in the general areas of systems and control, and signal processing. His current research interests include multirate systems, wavelet analysis, generalized sampling and reconstruction processes, and their applications in image processing.

Ruili Wang received the Ph.D. degree in computer science from Dublin City University, Dublin, Ireland.

He is a Professor of artificial intelligence in the Institute of Natural and Mathematical Sciences, Massey University, Wellington, New Zealand. His research interests include speech processing, image processing, data mining, intelligent systems, and complex systems. He is an Associate Editor or a member of the editorial boards of *Knowledge and Intelligent Systems*, *Health Information Science and Systems*, *Applied Soft Computing*, and *Complex and Intelligent Systems*.